Peculiar magnetocaloric properties and critical behavior in antiferromagnetic Tb_3Ni with complex magnetic structure

A. Herrero [a], A. Oleaga [a, *], A. F. Gubkin [b, c], A Salazar [a], N. V. Baranov [b, c]

[a] Departamento de Física Aplicada I, Escuela de Ingeniería de Bilbao, Universidad del País Vasco UPV/EHU, Plaza Torres Quevedo 1, 48013 Bilbao, Spain
[b] M.N. Miheev Institute of Metal Physics, Ural Branch of the Russian Academy of Sciences, 620108 Ekaterinburg, Russia
[c] Institute of Natural Sciences and Mathematics, Ural Federal University, 620083 Ekaterinburg, Russia

ABSTRACT

A study on the magnetocaloric properties of a Tb_3Ni single crystal (which crystallizes in the orthorhombic *Pnma* space group) has been undertaken and combined with the study of the character and critical behavior of its magnetic transitions. It presents two important magnetocaloric effects in the temperature range 3-90 K due to the richness and variety of its temperature and magnetic field induced phase transitions. There is a conventional (direct) magnetocaloric effect with a maximum at 65 K and very competitive properties: $\left|\Delta S_M^{pk}\right|$ = 16.6 J/kgK, RC_{FWHM} = 432 J/kg, with a 50 K span, for $\mu_0\Delta H$ = 5 T, which is due to the transition from magnetically ordered state to the paramagnetic (PM) state with a combined antiferromagnetic to ferromagnetic (AFM-FM) metamagnetic transition. Besides, it also presents an inverse magnetocaloric effect at very low temperature for which the presence of metamagnetic transitions between AFM and FM states is responsible (ΔS_M^{pk} =19.9 J/kgK, RC_{FWHM} = 245 J/kg, with a 15 K span, for $\mu_0\Delta H$ = 5 T). At low field (< 2 T), the character of the AFM-PM transition which takes place at ≈ 61 K has been well established to be second order and governed by short range order interactions, as the critical parameters α, A^+/A^- obtained from the specific heat at $\mu_0 H$ = 0 T point to the 3D-Heisenberg universality class. Conversely, the metamagnetic transitions between AFM and FM states, which appear for magnetic fields higher than 2 T, have a first order character, as proved by the magnetization behavior as a function of field and temperature. These properties make this material extremely interesting for magnetic refrigeration applications in the gas liquefaction range 4-77 K.

Keywords: Inverse magnetocaloric effect; direct magnetocaloric effect; Tb_3Ni; spin-ordering; critical behavior; thermal diffusivity

*Corresponding author; E-mail: alberto.oleaga@ehu.es

1. Introduction

A current wide field of research is the development of refrigeration devices based on alternative techniques to the traditional gas-compression refrigeration, looking for more environmentally friendly techniques to work, not only at room temperature, but also in the range of helium, hydrogen and nitrogen liquefaction (4-77 K), searching for higher thermal efficiencies as well. Magnetic refrigeration based on the magnetocaloric effect (MCE) is a most promising technique expected to strongly contribute to this end [1, 2]. Several candidate materials have been presented to work at (or near to) room temperature, mainly Gd-based [3-5] but also manganites [6], Heusler alloys [7, 8] and others [9, 10]. In the gas liquefaction range, different kind of materials have been found to have excellent properties, such as Laves Phases of the type RCo$_2$, RAl$_2$ (R = Ho, Dy, Er) or with minor substitutions for Co or even with mixed rare earths; ternary compounds such as RFeSi (R=Dy, Er, Tb and mixed rare earths) or the Gd$_5$(Si,Ge)$_4$ family also present relevant properties [1, 2, 11].

A giant magnetocaloric effect has been found to appear in materials with first order phase transitions (FOPT) but, as they present a relevant thermal and magnetic hysteresis, and the temperature span is thinner, they have limited practical application; therefore,a thorough search for magnetocaloric effects based on second order phase transitions (SOPT) is currently being developed, as they present a reversible MCE over a broader temperature range and thus higher refrigerant capacities. Besides, some of the high magnetic entropy changes spikes found in some FOPT-based magnetocaloric materials have been found to be spurious because of an incorrect application of the Maxwell relation to perform the calculations, showing that a correct evaluation of the entropy change gives lower values, though still highly competitive [12-16].

Most of those materials present the direct magnetocaloric effect (DMCE), based on transitions from a paramagnetic state (PM) to a ferromagnetic one (FM), for which the magnetic entropy is reduced when a magnetic field is adiabatically applied. Cooling is attained by the subsequent application of an adiabatic demagnetization [17]. In the last years a renovated interest is focused on materials which present an inverse magnetocaloric effect (IMCE), for which the magnetic entropy increases with an applied magnetic field and, therefore, cooling is obtained by adiabatic magnetization; this is the case for FOPT such as antiferromagnetic to ferromagnetic (AFM-FM), AFM-

ferrimagnetic transitions, or AFM-collinear/AFM-non-collinear [2, 7]. These materials can be used, not only for cooling, but as heat-sinks as well, for heat generated when a conventional magnetocaloric material is magnetized before cooling by adiabatic demagnetization [7, 18]. Along this line, materials which present, in a row, inverse and direct magnetocaloric effect are specially interesting for this kind of applications, as they can increase refrigeration efficiency [19, 20].

An intermetallic family which has been found to present very interesting magnetic properties is R_3TM (R=Gd, Dy, Tb; TM=Co, Ni). They have the highest contents of R among the general family R_nTM_m with the particularity that the transition metal ion does not carry a net magnetic moment for $n/m > 1$. Some of the members of the family have already been found to present magnetocaloric properties (Gd_3Co, Dy_3Co, Tb_3Co, Gd_3Ni) through a direct magnetocaloric effect, with values of the variation of the magnetic entropy and refrigeration capacity competitive in their respective temperature ranges [21-25].

Concerning Tb_3Ni, only a few studies have been performed since its crystallographic structure and magnetic properties were first studied [26], where it was found that Tb_3Ni belongs to the space group *Pnma*, that there is a magnetic transition to an antiferromagnetic state at about 62 K and that it presents magnetic anisotropies, with Tb occupying two non-equivalent positions (4*c* and 8*d* Wyckoff sites) which will lead to strong crystal-field effects. Electrical resistivity and specific heat have been measured as a function of temperature [27, 28] and a neutron diffraction study was performed together with magnetic measurements to prove the existence of short-range magnetic correlations in the paramagnetic state [29]. Finally, a very complete study on neutron diffraction and field-induced magnetic phase transitions in this material has been recently published, showing an extremely complex behavior: neutron diffraction data has shown that there is a transition from a paramagnetic phase at high temperature to an incommensurate magnetic phase at about 60 K, then (on lowering the temperature) to a lock-in, mixed magnetic phase with coexistence of incommensurate and lock-in components; finally, at about 46 K, there is a new transition to a commensurate antiferromagnetic phase. On applying magnetic fields, different metamagnetic transitions have been found to arise [30]. Nevertheless, the magnetocaloric properties of Tb_3Ni have not been studied yet, which is the main aim of the present study. At the same time, we will shed more light on the properties of the phase transitions through the study of their critical behavior by combining thermal and magnetic techniques.

2. Samples and Experimental Techniques

The sample is the same one as used in reference [30]. Tb_3Ni ingot was prepared by induction melting of terbium and nickel metals in a helium atmosphere using metallic Tb and Ni of 99.9% and 99.99% purity, respectively. Several single crystals with largest dimensions of approximately $4 \times 5 \times 6$ mm^3 were extracted from the ingot after slowly cooling the melt through the peritectic point. The quality and homogeneity of the single crystal were determined using x-ray Laue diffraction. Tb_3Ni, as it is well known, crystallizes in the *Pnma* space group [26, 30]. The final sample was prepared as a parallelepiped with its surfaces perpendicular to the three axis *a*, *b*, and c, with well polished surfaces.

Magnetization (M) measurements have been carried out in a VSM (Vibrating Sample Magnetometer) by Cryogenic Limited under external applied magnetic fields $\mu_0 H$ ranging from 0 to 6 T, all applied along the c direction. For the magnetocaloric studies, isotherms have been collected over a range of 3-130 K with $\Delta T = 1$ K between 35-76 K, $\Delta T = 2$ K between 3-35 K and 76-100 K and $\Delta T = 5$ K between 100-130 K. The isotherms have been collected starting at the lowest temperature, applying the magnetic field up to 6 T, then removing it, and moving to the next temperature, repeating the procedure till the last isotherm is acquired.

Thermal measurements have been performed using a high resolution *ac* photopyroelectric calorimeter in the back detection configuration. Thermal diffusivity has been measured from room temperature down to 30 K, paying special attention to the region around the magnetic transitions, where also specific heat has been retrieved, using slow temperature rates in order to acquire the shape of the transitions in detail, checking possible thermal hysteresis at the same time. This technique is customarily used to study the critical behavior in magnetic phase transitions in many materials, including intermetallics [25, 31-36], as it gives a high resolution. The details of the theory on how to extract the thermal variables from the photopyroelectric signal and the experimental setup can be found elsewhere [31, 32]. With this technique, thermal diffusivity is measured in a direction perpendicular to the surface, the direction *a* in this case.

3. Experimental results and Discussion

Fig. 1 shows the magnetization as a function of temperature where an antiferromagnetic transition is clearly observed at $T_N = 61 \pm 0.5$ K. This curve is perfectly comparable to the results obtained in previous studies [29, 30]. At $T < T_N$ some structure is also found

with a broad anomaly around 48 K (T_t, found in literature to correspond to the disappearance of the lock-in transition [30]), while there is a hysteretic behavior on heating and cooling.

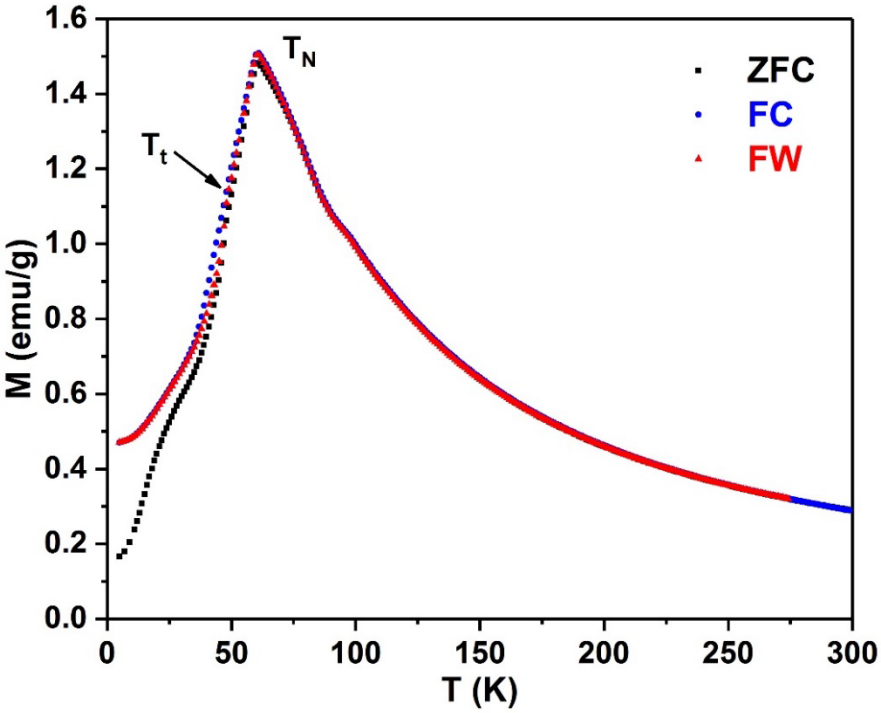

Fig. 1. Magnetization as a function of temperature Zero-field cooled (ZFC), field-warmed (FW) and field-cooled (FC) measured along the *c* axis with *H*=1 kOe.

Fig. 2 contains the thermal diffusivity curve obtained as a function of temperature, without any applied magnetic field, presenting typical characteristics of intermetallic materials. In intermetallics, heat is transferred both by electrons and by phonons. At high temperatures the electron contribution is dominant but this contribution is less and less relevant as temperature is lowered, which is why the thermal diffusivity is reduced [25, 35, 37, 38]. On the other hand, the phonon contribution becomes more important at low temperatures as the phonon mean free path increases. This value is highly increased in the ordered, AFM phase. The competition between one mechanism which loses relevance and the other one which gains it (and both of them might be of the same order of magnitude) [25, 34, 35, 39, 40] makes the thermal diffusivity present a well in many intermetallic materials, after which it quickly grows while temperature keeps on descending. In the inset of Fig. 2 the found phase transitions are indicated. The

antiferromagnetic transition is signalled by the change in slope at 59.96 ± 0.01 K, in agreement with magnetic measurements shown in Fig. 1, while the shoulder centered around 46 K is related to the disappearance of the lock-in transition at T_t [30]. There is no hint of thermal hysteresis in any of these transitions.

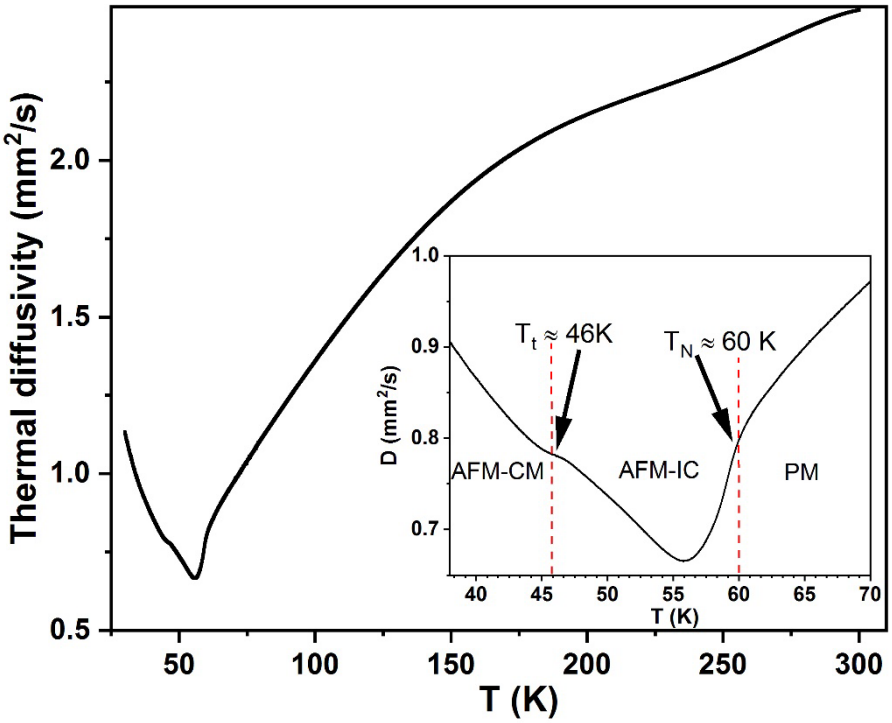

Fig. 2. Thermal diffusivity as a function of temperature. The inset indicates the temperatures at which magnetic phase transitions take place, where the phases have been labelled as indicated in literature [30]: T_t corresponds to the disappearance of the lock-in transition, T_N to the Néel temperature. AFM stands for antiferromagnetic phase, PM for paramagnetic, CM for commensurate, IC for incommensurate.

Fig. 3a shows the high resolution specific heat obtained in the phase transitions region, where a characteristic peak is found for the transition from the paramagnetic state to the magnetically ordered state. This is a second order phase transition, as declared by its shape and the absence of thermal hysteresis; therefore, it is possible to study its critical behavior to have more information about the order of the magnetic interactions (short or long-range) and the isotropical/anisotropical distribution of the spins.

Renormalization group theory applied to scaling analysis has established that specific heat fulfills, in the near vicinity of the critical temperature (T_N in this case) of a second-order phase transition, the following equation:

$$c_p = B + Ct + A^{\pm} |t|^{-\alpha} \left(1 + E^{\pm} |t|^{0.5}\right) \quad (1)$$

where t is the reduced temperature $t = (T-T_N)/T_N$, α is the critical exponent, and $A^{\pm}$, B, C and $E^{\pm}$ are adjustable parameters. Superscripts + and - stand for $T > T_N$ and $T < T_N$ respectively [32, 41, 42]. The parameters which hold physical meaning are the critical exponent α and the ratio A^+/A^-, whose values indicate whether the transition belongs to any of the theorized universality classes, each of them related to different magnetic properties. Table 1 summarizes the values for the most common universality classes in magnetic systems.

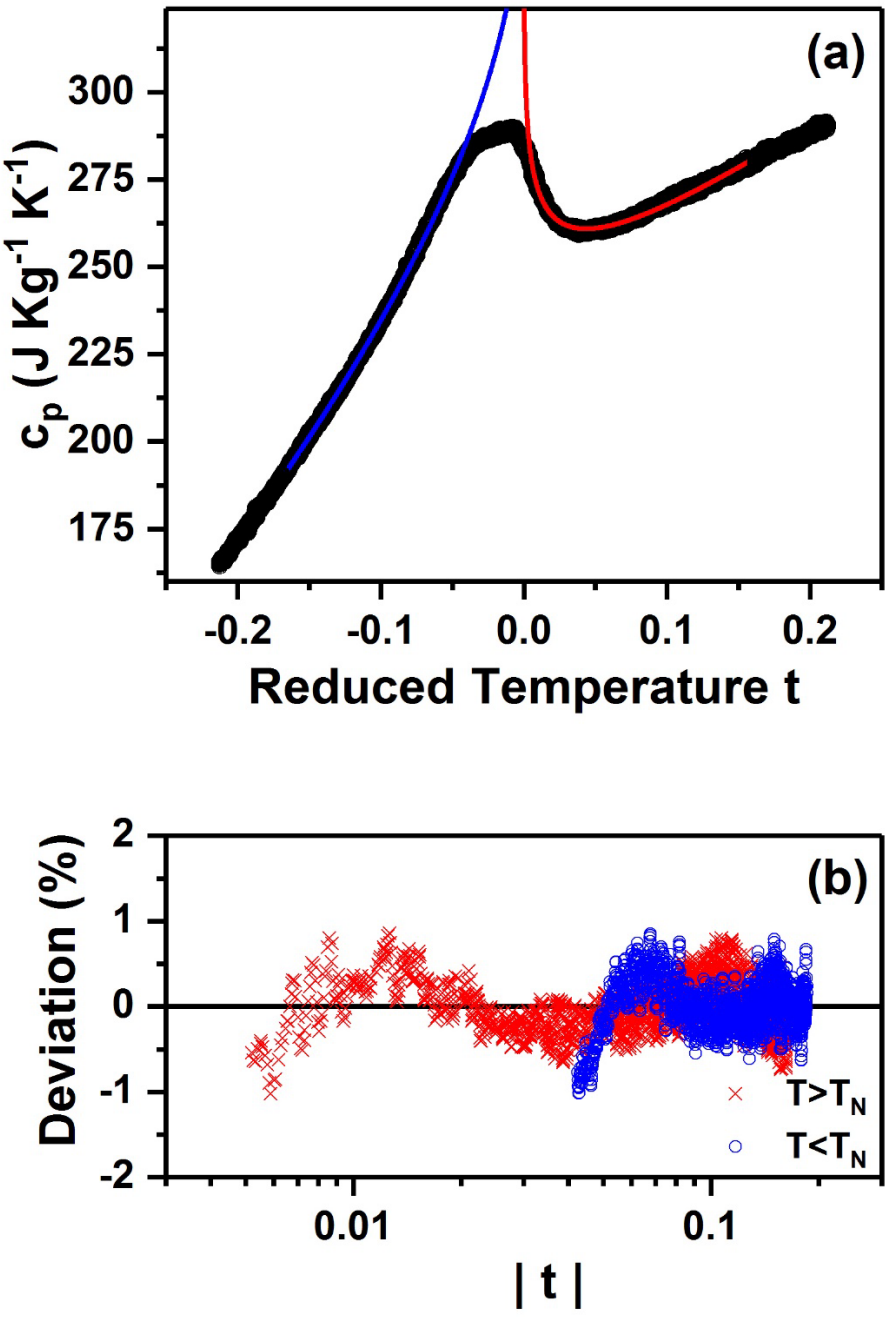

Fig. 3. a) Experimental specific heat (dots) together with the fitted functions (continuous curves) to equation (1), as a function of the reduced temperature $t = (T-T_N)/T_N$; b) Deviation plot: crosses for the region above the Néel temperature, circles for the region below

Table 1. Main universality classes for different magnetic systems [41, 43-46].

Universality class	***α***	A^+/A^-	***Order of the magnetic interactions & Spin arrangement***
Mean-field Model	0	-	Long-range order
3D-Ising	0.11	0.53	Short-range order Uniaxial anisotropy
3D-XY	-0.014	1.06	Short-range order Easy plane
3D-Heisenberg	-0.134	1.52	Short-range order Isotropy

Fig. 3a presents the best fitting of the experimental points to Eq. (1) (the detailed fitting procedure can be found elsewhere [47]), with the result that $\alpha = -0.13 \pm 0.02$ while $A^+/A^- = 2.15$. Fig. 3b contains the deviation plot (difference between the fitted and the experimental points, in percentage), which indicates the points used for the fitting (avoiding the rounded section, as is customary) and its good quality. The value of the critical exponent clearly points to the 3D-Heisenberg, short-range, isotropic model but the ratio deviates from the theoretical value. This kind of deviations indicate that there is not a perfect isotropic distribution of spins, surely due to crystal-field effects, provoked by the Tb occupancy of low-symmetry sites in the orthorhombic lattice, which have been found to affect the magnetic properties of R_3TM in general and of Tb_3Ni in particular [29, 48-50]; nevertheless, they are not important enough to reach an easy-plane or an easy-axis distribution of spins, as neither the 3D-XY nor the 3D-Ising universality classes are of application. This is in agreement with the magnetic anisotropic measurements performed in [30] where it was shown that magnetization was easier along the *c* axis than along *a* or *b* around the Néel temperature but that only at very low temperature *c* became an easy axis. The fact that this transition nearly belongs to the 3D-Heisenberg class also assesses that the magnetic interactions are short-range, corroborating the results previously obtained by means of neutron diffraction that sort-range order interactions were present even in the paramagnetic phase at temperatures high above T_N [29, 30]. Short-range order interactions have also been found in other members of the R_3TM family [21, 36].

In order to study the magnetocaloric properties of Tb_3Ni, the magnetic field-induced isothermal entropy change, ΔS_M must be evaluated [17]. An indirect method based on the acquisition of isothermal $M(H)_T$ magnetization measurements has been used to this end. For the case of SOPT the entropy change can be obtained from the Maxwell relation:

$$\Delta S_M(\mathrm{T}, \Delta\mathrm{H}) = \mu_0 \int_{H_i}^{H_f} \left(\frac{\partial M}{\partial T} \right)_H dH \qquad (2)$$

where M is magnetization, T temperature, H magnetic field, μ_0 magnetic permeability of vacuum. The integral is performed between the extreme values of the applied magnetic field H_i, H_f. On the other hand, for a FOPT the use of this equation may lead to incorrect results and spurious peaks, overestimating the change in magnetic entropy, as commented in the introduction.

In the case of Tb_3Ni, the application of magnetic field leads to quite a complex behavior, revealing different metamagnetic transitions with a critical field depending on temperature. Fig. 4 shows the magnetization as a function of temperature in the region of interest with applied fields up to 6 T (the data have been taken from the isotherms). At very low temperature, a field-induced metastable ferromagnetic phase appears at even zero field due to the fact that, once the field is removed after the first isotherm is collected (which takes the sample to a FM phase), the system stays in that state [30]. Increasing the temperature up to ≈ 10 K eliminates this metastable FM state and, from that temperature onwards, after having acquired each isotherm and removed the magnetic field, the sample returns to the AFM state. The magnetic field application turns this AFM state, below the Néel temperature, into a metamagnetic FM state. This development takes place at different fields, depending on the temperature regions.

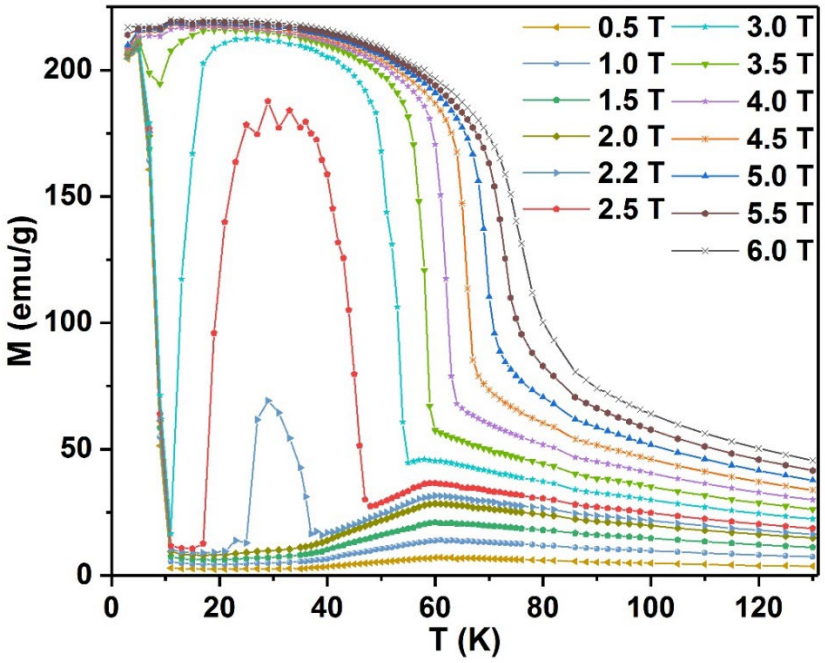

Fig. 4. Magnetization as a function of temperature for different applied external fields.

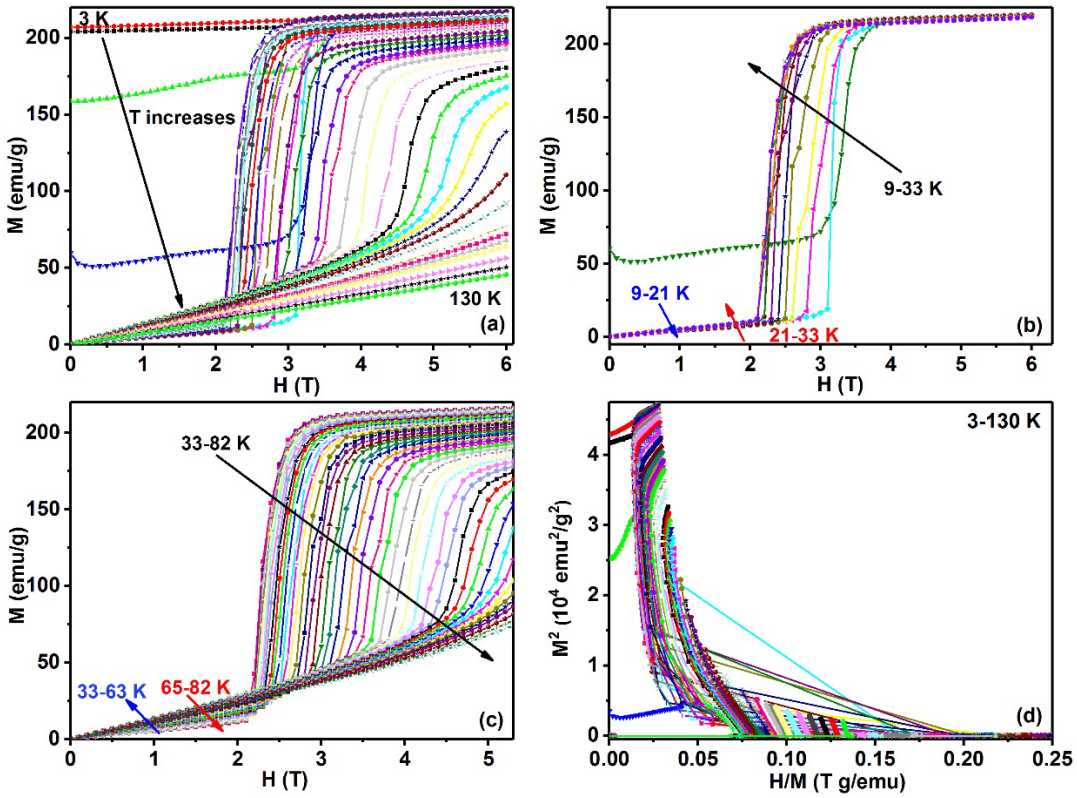

Fig 5 (a) Magnetization as a function of the applied magnetic field for selected isotherms in the range 3 to 130 K; (b) detail from 9 to 33 K; (c) detail from 33 to 82 K; (d) Arrot plot for the range 3 to 130 K. The arrows indicate the direction of increasing temperatures.

Fig. 5(a) contains isotherms measured from 3 to 130 K (not all of them have been drawn, for the sake of clarity) where it is clearly seen that the behavior is very complex, showing the presence of several metamagnetic transitions. Fig 5(b) and 5(c) show the detail in different temperature and field regions. From Figs. 5(a)-(b) it can be appreciated that, at very low temperatures, the system is in the metastable FM state which turns into an AFM state (achieved at 11 K) as temperature is increased, at fields lower than 2 T. If $\mu_0 H$ is increased to values higher than roughly 2 T, then a clearly FOPT metamagnetic transition to a FM state appears but it is mixed with the AFM phase in the sense that as temperature increases, for the same value of the field at high fields, magnetization increases while, for low fields, it decreases. This situation changes in the region 21-33 K (see Fig. 5(b)), where, at low fields, the evolution of the curves is completely in agreement with an AFM state (magnetization increases with temperature) and there is a metamagnetic transition to the FM state. Fig. 5(c) shows the region between 33 and 82 K. A metamagnetic transition to a pure FM state takes place at fields higher than 2 T, while, at lower fields (roughly < 2 T), there are two regions: up to 63 K the behavior is AFM, while from 63 K upwards the magnetization, at a given field, decreases with temperature. This sequence of transitions is in agreement with the phase diagram previously found for Tb_3Ni [30].

Finally, Fig 5(d) shows the Arrott plot where it is clearly seen that the slopes of the curves are negative in a region which corresponds to applied fields higher than 2 T, indicating, after the Banerjee criterion [51], that the metamagnetic transitions have a first order character.

From the shape of the magnetization curves (Figs. 5(a)-(b)) it is also clear that in the metamagnetic transitions there is a clear coexistence of the FM and AFM phases up to 33 K, as they present a marked stepwise magnetic behavior [13, 15, 16] (specially marked at low temperatures), while from there on this behavior is still present, though in a much lesser degree.

Therefore, due to the first order character of these metamagnetic transitions, the use of the Maxwell relation (Eq. (2)) is not adequate to calculate the magnetic entropy change as it leads to an overestimation because, whenever there is a FOPT, Eq (2) would include not only the contribution to the change in magnetization as a result of the orientation of the magnetic moments in an applied field, but also as the result of the relative change in the fractions of the two coexisting phases. For a proper calculation in the last case, the Clausius-Clapeyron equation must be used, instead [13, 16, 52-54].

$$\Delta S_M^{CC}(\mathrm{T},\mathrm{H}_c) = -\mu_0 \Delta M \frac{dH_C}{dT} \quad (3)$$

where $\Delta S_M^{CC} = S_M^B - S_M^A$, $\Delta M = M^B - M^A$ are the gaps of the magnetic entropy change and magnetization of the coexisting phases A and B, while H_C is the critical field.

Following Caballero Flores *et al* [52], we will then obtain the magnetic entropy change by independently calculating ΔS_M for the range of temperatures and magnetic fields inside the transition region using the Clausius-Clapeyron equation and, outside this region, using the Maxwell relation. The extent of the transition region is very clear for $T < 33$ K (see Fig. 5(b)). For $T > 33$ K (Fig. 5(c)) we have taken as the beginning and end of the transition region the inflection points in the isothermal magnetizations. H_C has been taken as the critical field value of the inflection point within the metamagnetic transitional region [13] and its variation with temperature is shown in Fig. 6, together with a polynomial fit, from where the first derivative $\frac{dH_C}{dT}$ has been retrieved. In the low temperature region ($T <$ 11 K), we have additionally followed the procedure commonly used for stepwise behavior, where only the contribution to the magnetic entropy change of the final phase is taken into account when considering the area between two particular isotherms [15, 16, 53].

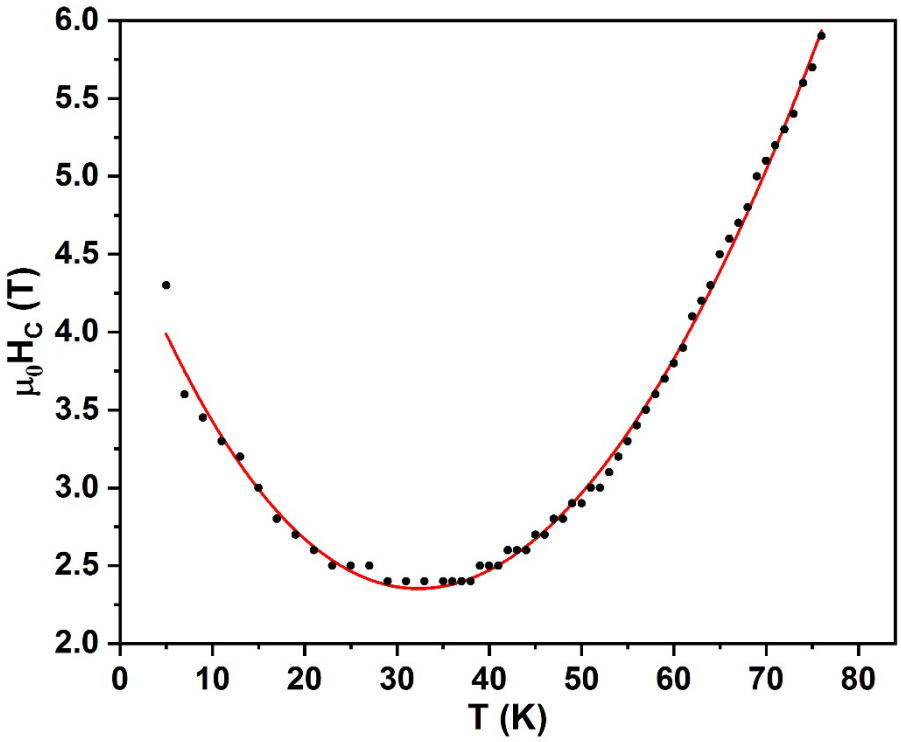

Fig 6. Critical Field for the metamagnetic transition to take place, as a function of temperature. The dots represent the points retrieved from the measurements while the continuous line is a polynomial fit.

The total magnetic entropy change with $\mu_0\Delta H$ from 0 to 6 T is shown in Fig. 7, where it can be seen that there are two magnetocaloric effects, an inverse one at low temperature and a direct one at a higher one. Fig. 8 shows the detail with $\mu_0\Delta H$ from 0.1 to 2.1 T, before the metamagnetic transitions take place. In this field region, the magnetic entropy change presents the typical behavior corresponding to an AFM-PM transition, with an inversion in the magnetic entropy change just below the Néel temperature and with a maximum developing at higher fields and moving to lower temperatures, as theoretically predicted and verified in other materials [55-57]. At higher fields (see Figs. 4 and 6) the metamagnetic transitions take place, leading to two important magnetocaloric effects, a direct one with a maximum at about 65 K, and an inverse one, with a maximum at about 11 K. The insert in Fig. 7 shows $-\Delta S_M$ as a function of $\mu_0\Delta H$ at 52 K, indicating how the field induced metamagnetic transition turns what would have been a small IMEC into the relevant DMCE.

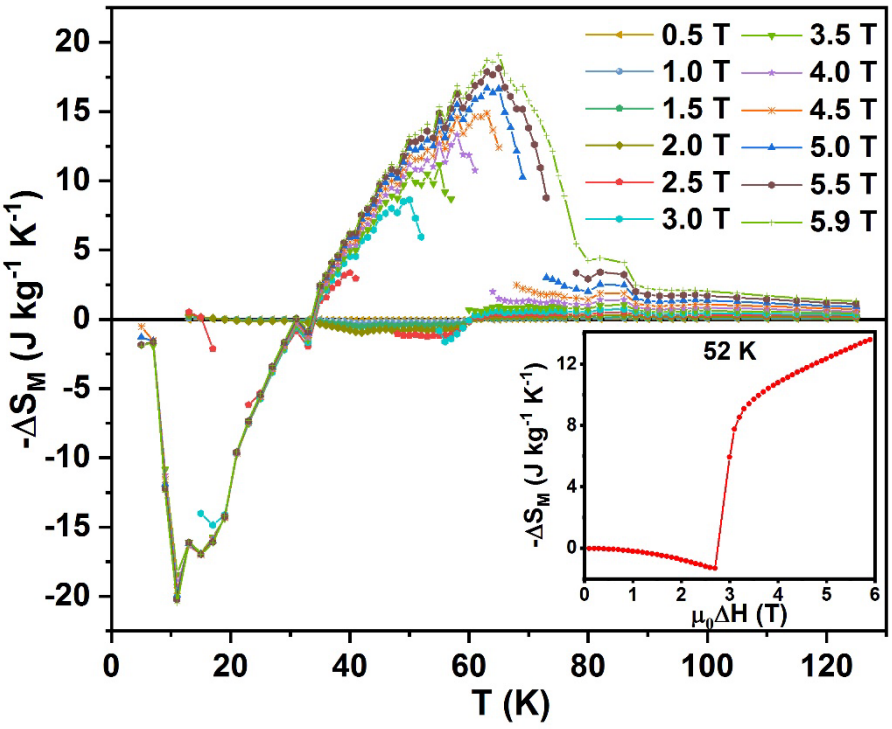

Fig. 7. Magnetic entropy change $-\Delta S_M$ for $\mu_0 \Delta H$ from 0.5 T to 5.9 T. Insert: $-\Delta S_M$ as a function of $\mu_0 \Delta H$ at 52 K.

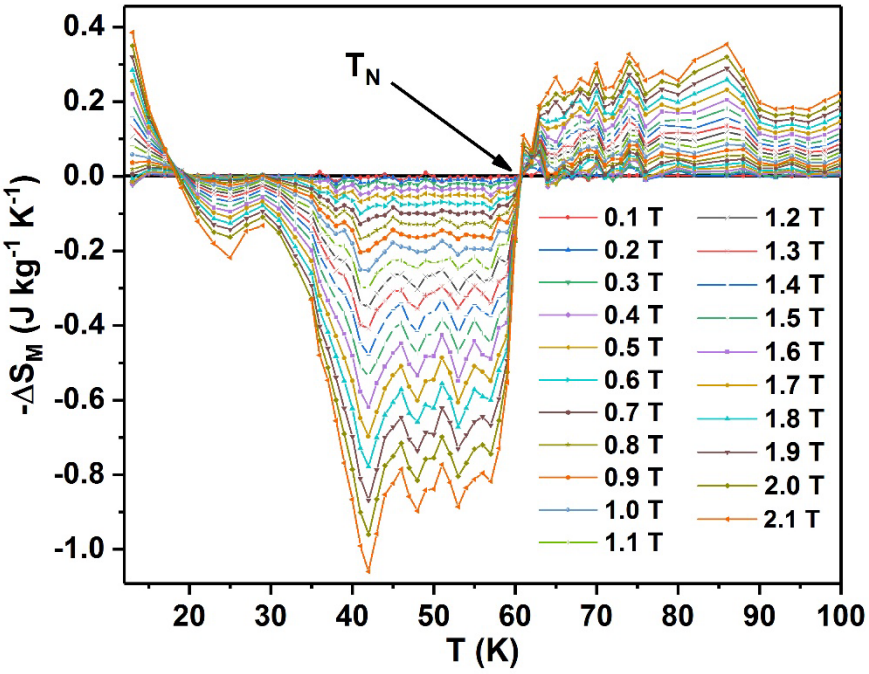

Fig. 8. Magnetic entropy change for $\mu_0 \Delta H$ from 0.1 T to 2.1 T.

In the case of the direct effect, with an increasing applied field, there is an inversion of the sign of the magnetic entropy change which starts in the region 33-40 K and grows to higher temperatures, developing a very wide magnetic entropy peak, whose maximum stabilizes at about 65 K from an applied field of 5 T upwards. In the case of the inverse effect, it is the metastable ferromagnetic part at low temperature which, as it becomes antiferromagnetic, feeds the magnetic entropy change peak with a maximum which is displaced to lower temperatures till it is fixed at 11 K for 3.5 T.

The values of the maximum entropy and the refrigerant capacity are extremely competitive in their respective temperature ranges, especially for the DMCE. For $\mu_0 \Delta H$ = 5 T, $\left|\Delta S_M^{pk}\right|$ = 16.6 J/kgK at 65 K, in the highest region of values shown in Fig. 25 of the recent review published by Franco *et al* [1], where a very thorough revision of materials is done. Concerning the refrigerant capacity, this is customarily defined in two ways: RC_{FWHM} is calculated as the product of $\left|\Delta S_M^{pk}\right|$ times the width of ΔS_M at half maximum, while RC_{Area} is the area enclosed by the ΔS_M vs. temperature curves in the temperature range enclosed by the full width at half maximum of the peak. For Tb_3Ni, in the DMCE, RC_{FWHM} = 432 J/kg, RC_{Area} =341 J/kg which are extremely high values and with the added advantage that the width of the magnetocaloric effect is very wide. For the IMCE, ΔS_M^{pk} =19.9 J/kgK, at 11 K, also for $\mu_0 \Delta H$ = 5 T. In this temperature region, the comparison with the materials published in the mentioned review [1] is not as good as in the other case but its value is also quite high, while RC_{FWHM} = 245 J/kg and RC_{Area} =194 J/kg.

Finally, the results obtained from the magnetic measurements at low field confirm what was extracted from the thermal measurements about the character of the AFM-PM transition (before the metamagnetic transition appears), that it is second order. This is further confirmed because a universal master curve can be built up for the normalized ΔS_M curves below the critical field H_C, where all data collapse. In the case of the conventional magnetocaloric effect, such kind of universal curve is attained when ΔS_M is normalized to its peak value and the temperature is rescaled using one or two reference temperatures T_r [5, 58, 59]. But it has been shown that, in the case of an IMCE in an AFM-PM second order phase transition, there is no need to rescale the temperature [57]. Fig. 9 shows that there is a very good collapse below 2 T without the use of any reference temperature to rescale this variable.

Concerning the metamagnetic transition which takes place on the application of higher fields, there is still another method (apart from the Banerjee criterion discussed on Fig. 5d) to check its character, using the evolution of the exponent n of the field dependence of ΔS_M with temperature $n(T,H) = \frac{d \ln |\Delta S_M|}{d \ln H}$. This exponent must have a value of 2 in the paramagnetic phase while, in the case of a first order phase transition, there should be a shoot well above this value, tending to 1 at temperatures well below the critical one [60, 61]. Fig. 10 shows n for Tb_3Ni, for $\mu_0 \Delta H$ = 3.5 T. There is a clear overshoot at the metamagnetic transition at 61 K, proving that it is first order. In the region shadowed in grey there is a dip at 31 K which is due solely to the change in sign in ΔS_M [20]. At the lower phase transition, another spike starts to form due to the metamagnetic transition responsible for the IMCE but there are not enough experimental points to see it clearly developed.

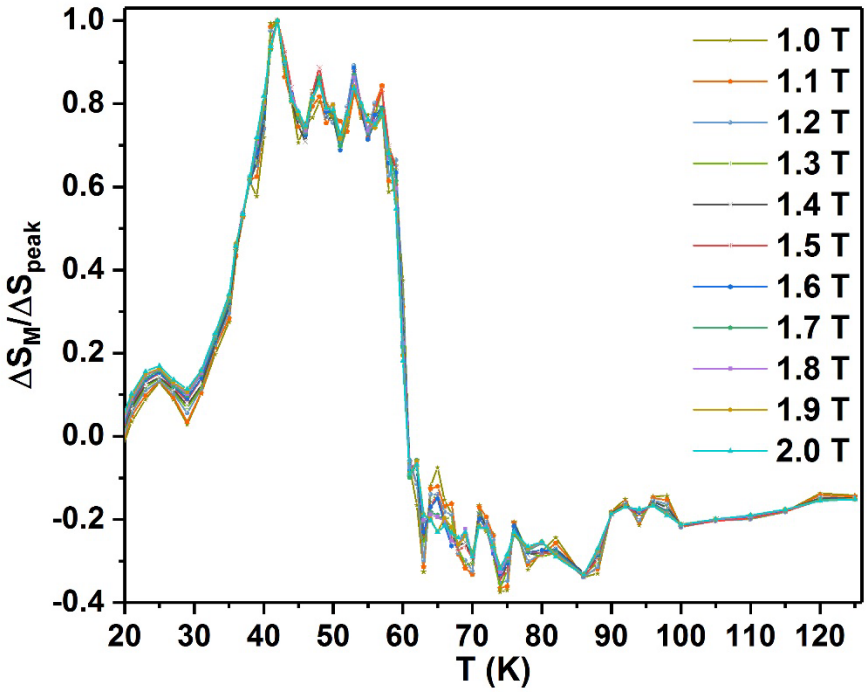

Fig. 9. Universal master curve for $\mu_0 \Delta H$ from 1 T to 2 T

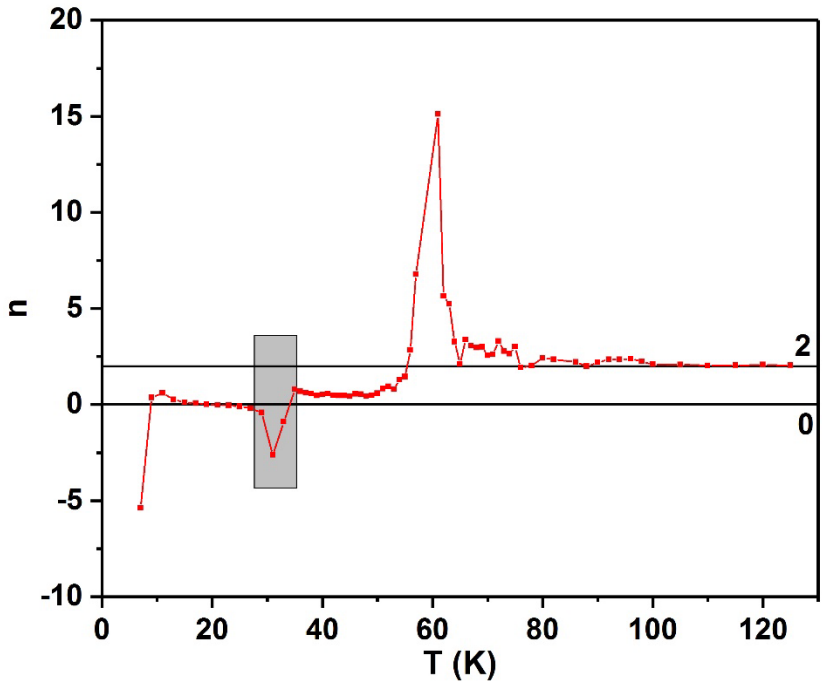

Fig. 10. *n(T)* for $\mu_0\Delta H$ = 3.5 T. The shoot at 61 K proves the character of the transition to be first order. The dip in the shadowed region is simply due to the change in sign of the magnetic entropy change.

Conclusions

Tb_3Ni presents two important magnetocaloric effects due to the very complex phase diagram which includes different temperature and field induced phase transitions. There is an inverse magnetocaloric effect with a maximum for the magnetic entropy change at 11 K, mainly due to the metamagnetic transition between AFM and FM states (ΔS_M^{pk} =19.9 J/kgK, RC_{FWHM} = 245 J/kg for $\mu_0\Delta H$ = 5 T) and a direct one with its maximum at 65 K ($\left|\Delta S_M^{pk}\right|$ = 16.6 J/kgK, RC_{FWHM} = 432 J/kg, with a 50 K span, for $\mu_0\Delta H$ = 5 T) due to the transition to the PM state with a combined AFM-FM metamagnetic transition. At low field (< 2 T), the character of the AFM-PM transition has been well established to be second order and governed by short range order interactions, without a clear spin orientation preference, while the metamagnetic transitions (with critical fields which are temperature dependent but higher than 2 T) have been shown to be first order. These properties make this material extremely interesting for magnetic refrigeration applications in the gas liquefaction range 4-77 K.

Acknowledgements

This work has been supported by Universidad del País Vasco UPV/EHU (GIU16/93). A. Herrero thanks the Department of Education of the Basque Government as grantee of the programme "Programa Predoctoral de Formación de Personal Investigador No Doctor". The authors thank for technical and human support provided by SGIker of UPV/EHU. This work was also supported by Russian Science Foundation (project No. 18-72-10022).

REFERENCES

[1] V. Franco, J.S. Blázquez, J.J. Ipus, J.Y. Law, L.M. Moreno-Ramírez, A. Conde, Magnetocaloric effect: From materials research to refrigeration devices, Progress in Materials Science 93 (2018) 112-232.

[2] H. Zhang, R. Gimaev, B. Kovalev, K. Kamilov, V. Zverev, Review on the materials and devices for magnetic refrigeration in the temperature range of nitrogen and hydrogen liquefaction, Phys. B: Condensed Matter 558 (2019) 65-73.

[3] V.K. Pecharsky, K.A. Gschneider, Giant magnetocaloric effect in $Gd_5Si_2Ge_2$, Jr. Phys. Rev. Lett. 78 (1997) 4494-4497.

[4] S. Couillaud, E. Gaudin, V. Franco. A. Conde, R. Pöttgen, B. Heying, U.Ch. Rodewald, B. Chevalier, The magnetocaloric properties of GdScSi and GdScGe, Intermetallics 19 (2011) 1573-1578.

[5] A. Herrero, A. Oleaga, P. Manfrinetti, A. Provino, A Salazar, "Study of the magnetocaloric effect in intermetallics RTX (R = Nd, Gd; T = Sc, Ti ; X = Si, Ge), Intermetallics 110 (2019) 106495.

[6] Z.B. Guo, Y.W. Du, J.S. Zhu, H. Huang, W.P. Ding, D, Feng, Large Magnetic Entropy Change in Perovskite-Type Manganese Oxides, Phys. Rev. Lett. 78 (1997) 1142-1145.

[7] T. Krenke, E. Duman, M. Acet, E.F. Wassermann, X. Moya, L. Mañosa, A. Planes, Inverse magnetocaloric effect in ferromagnetic Ni-Mn-Sn alloys, Nature Materials 4 (2005) 450-454.

[8] F. Hu, B. Shen, J. Sun, Magnetic entropy change in $Ni_{51.5}Mn_{22.7}Ga_{25.8}$ alloy, Appl. Phys. Lett. 76 (2000) 3460-3462.

[9] A. Fujita, S. Fujieda, Y. Hasegawa, K. Fukamichi, Intinerant-electron metamagnetic transition and large magnetocaloric effects in $La(Fe_xSi_{1-x})_{13}$ compounds and their hydrides, Phys. Rev. B 67 (2003) 104416.

[10] H. Wada, Y. Tanabe, Giant magnetocaloric effect of $MnAs_{1-x}Sb_x$, Appl. Phys. Lett 79 (2001) 3302-3304.

[11] H. Zhang, Y.J. Sun, E. Niu, L.H. Yang, J. Shen, F.X. Hu, J.R. Sun, B.G. Shen, "Large magnetocaloric effects of RFeSi (R = Tb and Dy) compounds for magnetic refrigeration in nitrogen and natural gas liquefaction, Appl. Phys. Lett. 103 (2013) 202412.

[12] L. Tocado, E. Palacios, R. Burriel, Entropy determinations and magnetocaloric parameters in systems with first-order transitions: Study of MnAs, J. Appl. Phys. 105 (2009) 093918.

[13] M. Balli, D. Fruchart, D. Gignoux, R. Zach, The colossal magnetocaloric effect in $Mn_{1-x}Fe_xAs$: What are we really measuring?, Appl. Phys. Lett. 95 (2009) 072509.

[14] A. Giguere, M. Foldeaki, B. Ravi Gopal, R. Chahine, T.K. Bose, A. Frydman, J.A. Barclay, Direct measurement of the Giant adiabatic temperature change in $Gd_5Si_2Ge_2$, Phys. Rev. Lett. 83 (1999) 2262-2265.

[15] J.D. Zou, B.G. Shen, B. Gao, J. Shen, J.R. Sun, The magnetocaloric effect of $LaFe_{11.6}Si_{1.4}$, $La_{0.8}Nd_{0.2}Fe_{11.5}Si_{1.5}$, and $Ni_{43}Mn_{46}Sn_{11}$ compounds in the vicinity of the first-order transition, Adv. Mater. 21 (2009) 693-696.

[16] G.J. Liu, J.R. Sun, J. Shen, B. Gao, H.W. Zhang, F.X. Hu, B.G. Shen, Determination of the entropy changes in the compounds with a first-order magnetic transition, Appl. Phys. Lett 90 (2007) 032507.

[17] A.M. Tishin, Y.I. Spichkin, The Magnetocaloric Effect and its Applications, Series in Condensed Matter Physics, Institute of Physics Publishing, Bristol and Philadelphia (2003).

[18] A. Biswas, T. Samanta, S. Banerjee, I. Das, Inverse magnetocaloric effect in polycrystalline $La_{0.125}Ca_{0.875}MnO_3$, J. Phys. Condens. Matter 21 (2009) 506005 (3 pp).

[19] L.V.B. Diop, O. Isnard, Inverse and normal magnetocaloric effects in $LaFe_{12}B_6$, J. Appl Phys. 119 (2018) 213904.

[20] J.Y. Law, V. Franco, A. Conde, S.J. Skinner, S.S. Pramana, Modification of the order of the magnetic phase transition in cobaltites without changing their crystal space group, J. Alloy. Comp. 777 (2019) 1080-1086.

[21] J. Shen, J.L. Zhao, F.X. Hu, G.H. Rao, G.Y. Liu, J.F. Wu, Y.X. Li, J.R. Sun, B.G. Shen, Magnetocaloric effect in antiferromagnetic Dy_3Co compound, Appl. Phys. A 99 (2010) 853-888.

[22] S.K. Tripathy, K.G. Suresh, A.K. Nigam, A comparative study of the magnetocaloric effect in Gd_3Co and Gd_3Ni, J. Magn. Magn. Mater. 206 (2006) 24-29.

[23] B. Li, J. Du, W.J. Ren, W.J. Hu, Q. Zhang, D. Li, Z.D. Zhang, Large reversible magnetocaloric effect in Tb_3Co compound, Appl. Phys. Lett. 92 (2008) 242504 (3 pp).

[24] J.C.B. Monteiro, G.A. Lombardi, R.D. doe Reis, H.E. Freitas, L.P. Cardoso, A.M. Mansanares, F.G. Gandra, Heat flux measurements of Tb_3M series (M=Co, Rh and Ru): Specific heat and magnetocaloric properties, Physica B 503 (2016) 64-69.

[25] A. Herrero, A. Oleaga, A.F. Gubkin, M.D. Frontzek, A. Salazar, N.V. Baranov, Comprehensive study of the magnetic phase transitions in Tb3Co combining thermal, magnetic and neutron diffraction measurements, Intermetallics 111 (2019) 106519.

[26] D. Gignoux, J.C. Gomez-Sal, D. Paccard, Magnetic properties of a Tb_3Ni single crystal, Solid State Comm. 44 (1982) 695-700.

[27] E. Talik, Magnetic and transport properties of the R_3Ni system (R=Y, Gd, Tb, Dy, Ho, Er), Phys. B 193 (1994) 213-220.

[28] N. V. Tristan, K. Nenkov, K. P. Skokov, T. Palewski, Specific heat and magnetic susceptibility of intermetallic compounds R_3Ni, Phys. B 344 (2004) 462-469.

[29] N.V. Baranov, A.V. Proshkin, A.F. Gubkin, A. Cervellino, H. Michor, G. Hilscher, E.G. Gerasimov, G. Ehlers, M. Frontzek, A. Podlesnyak, Enhanced survival of short-range magnetic correlations and frustrated interactions in R_3T intermetallics, J. Magn. Magn. Mater. 324 (2012) 1907-1912.

[30] A.F. Gubkin, L.S. Wu, S.E. Nikitin, A.V. Suslov, A. Podlesnyak, O. Prokhnenko, K. Prokes, F. Yokaichiya, L. Keller, N.V. Baranov, Field.induced magnetic phase transitions and metastable states in Tb_3Ni, Phys. Rev. B 97 (2018) 134425.

[31] U. Zammit, M. Marinelli, F. Mercuri, S. Paoloni, F. Scudieri, Photopyroelectric calorimeter for the simultaneous thermal, optical, and structural characterization of samples over phase transitions, Rev. Scient. Inst. 82 (2011) 121101 (22 pp).

[32] M. Marinelli, F. Mercuri, D. P. Belanger, Specific heat, thermal diffusivity, and thermal conductivity of **FeF2** at the Néel temperature, Phys. Rev. B 51(1995) 8897.

[33] A. Oleaga, V. Shvalya, V. Liubachko, G. Balakrishnan, L.D. Tung, A. Salazar, Critical behavior study of the spin ordering transition in RVO3 (R = Ce, Pr, Nd, Sm, Gd, Er) by means of ac photopyroelectric calorimetry, J. Alloy. Comp. 703 (2017) 210-215.

[34] A. Herrero, A. Oleaga, P. Manfrinetti, A. Provino, A. Salazar, Critical behavior of the ferromagnetic transition in GdSc(Si,Ge) intermetallic compounds, Intermetallics 101 (2018) 64-71.

[35] A. Oleaga, V. Liubachko, P. Manfrinetti, A. Provino, Yu. Vysochanskii, A. Salazar, Critical behavior study of NdScSi, NdScGe intermetallic compounds J. Alloy. Comp. 723 (2017) 559-566.

[36] A. Herrero, A. Oleaga, A. Salazar, A.F. Gubkin, N.V. Baranov, Critical behavior of magnetic transitions in Dy_3Co single crystal, J. Alloy. Comp. 741 (2018) 1163-1168.

[37] C. Zanotti, P. Giuliania, G. Rivaa, A. Tuissi, A. Chrysanthouc, Thermal diffusivity of Ni–Ti SMAs**,** J. Alloy. Comp. 473 (2009) 231–237.

[38] A.O. Oliynyk, T.D. Sparks, M.W. Gaultois, L. Ghadbeigi, A. Mar, $Gd_{12}Co_{5.3}Bi$ and $Gd_{12}Co_5Bi$, Crystalline Doppelgänger with Low Thermal Conductivities, Inorg. Chem. 55 (2016) 6625−6633.

[39] A.K. Bashir, M.B.T. Tchokonté, A.M. Strydom, Electrical and thermal transport properties of $RECu_4Au$ compounds, RE=Nd, Gd, J. Magn. Magn. Mater. 414 (2016) 69-73.

[40] A. Kowalczyk, M. Falkowski, Thermal conductivity of $CeNiAl_4$ Kondo lattice, Intermetallics 37 (2013) 65-68.

[41] H.E. Stanley, Introduction to phase transitions and critical phenomena, Oxford University Press (1971).

[42] A. Oleaga, A. Salazar, D. Prabhakaran, J.G Cheng, J.S Zhou, Critical behavior of the paramagnetic to antiferromagnetic transition in orthorhombic and hexagonal phases RMnO3 (R=Sm, Tb, Dy, Ho, Er, Tm, Yb, Lu, Y), Phys. Rev. B 85 (2012) 184425.

[43] R. Guida, J. Zinn-Justin, Critical Exponents of the N-vector model, J. Phys. A: Math. Gen. 31 (1998) 8103-8121.

[44] M. Campostrini, M. Hasenbusch, A. Pelissetto, P. Rossi, E. Vicari, Critical behavior of the three-dimensional XY universality class, Phys. Rev. B 63 (2001) 214503.

[45] M. Campostrini, M. Hasenbusch, A. Pelissetto, P. Rossi, E. Vicari, Critical exponents and equation of state of the three-dimensional Heisenberg universality class, Phys. Rev. B 65 (2002) 144520.

[46] M. Hasenbusch, Universal amplitude ratios in the three-dimensional Ising universality class, Phys. Rev. B 82 (2010) 174434.

[47] A. Oleaga, A. Salazar, D. Skrzypek, Critical behaviour of magnetic transitions in $KCoF_3$ and $KNiF_3$ perovskites, J. Alloy. Comp. 629 (2015) 178-183.

[48] N.V. Baranov, A.F. Gubkin, A.P. Vokhmyanin, A.N. Pirogov, A. Podlesnyak, L. Keller, N.V. Mushnikov, M.I. Bartashevich, High-field magnetization and magnetic structure of Tb_3Co J. Phys. Condens. Matter 19 (2007) 326213 (14 pp).

[49] A.F. Gubkin, A. Podlesnyak, N.V. Baranov, Single-crystal neutron diffraction study of the magnetic structure of Er_3Co, Phys. Rev. B 82 (2010) 012403 (4 pp).

[50] A. Podlesnyak, A. Daoud-Aladine, O. Zaharko, P. Markin, N. V. Baranov, Magnetic structures and magnetic phase transitions in Ho_3Co, J. Magn. Magn. Mater. 272-276 (2004) 565-567.

[51] S.K. Banerjee, On a generalized approach to first and second order magnetic transitions, Phys. Lett. 12 (1964) 16-17.

[52] R. Caballero-Flores, N.S. Bingham, M.H. Phan, M.A. Torija, C. Leighton, V. Franco. A. Conde, T.L. Phan. S.C. Yu, H. Srikanth, Magnetocaloric effect and critical behavior in $Pr_{0.5}Sr_{0.5}MnO_3$: an analysis of the validity of the Maxwell relation and the nature of the phase transition, J. Phys. Condens. Matter 26 (2014) 286001.

[53] W. Cui, W. Liu, Z. Zhang, The origin of large overestimation of the magnetic entropy changes calculated directly by Maxwell relation, Appl. Phys. Lett. 96 (2010) 222509.

[54] J.S. Amaral, V.S. Amaral, On estimating the magnetocaloric effect from magnetization measurements, J. Magn. Magn. Mater. 322 (2010) 1552-1557.

[55] P.J. von Ranke, N.A. de Oliveira, B.P. Alho, E.J.R. Plaza, V.S.R. de Sousa, L. Caron, M.S. Reis, Understanding the inverse magnetocaloric effect in antiferro- and ferromagnetic arrangements, J. Phys. Condens. Matter 21 (2009) 056004 (8pp).

[56] L. Li, K. Nishimura, G. Usui, D, Huo, Z. Qian, Study of the magnetic properties and magnetocaloric effect in RCo_2B_2 (R=Tb, Dy and Ho) compounds, Intermetallics 23 (2012) 101-105.

[57] A. Biswas, S. Chandra, T. Samanta, M.H. Phan, I. Das, The universal behavior of inverse magnetocaloric effect in antiferromagnetic materials, J. Appl. Phys. 113 (2013) 17A902 (3 pp).

[58] V. Franco, A. Conde, J.M. Romero-Enrique, J.S. Blázquez, A universal curve for the magnetocaloric effect: an analysis based on scaling relations, J. Phys. Condens. Matter 20 (2008) 285207 (5pp).

[59] V. Franco, J.S. Blázquez, A. Conde, Field dependence of the magnetocaloric effect in materials with a second order phase transition: A master curve for the magnetic entropy change, Appl. Phys. Lett. 89 (2006) 222512.

[60] J.Y. Law, V. Franco, L.M. Moreno-Ramírez, A. Conde, D.Y. Karpenkov, I. Radulov, K.P. Skokov, O. Gutfleisch, A quantitative criterion for determining the order of magnetic phase transitions using the magnetocaloric effect, Nat. Comm. 9 (2018) 2680 (8 pp).

[61] L.M. Moreno-Ramírez, C. Romero-Muñiz, J.Y. Law, V. Franco, A. Conde, I. Radulov, F. Maccari, K.P. Skokov, O. Gutfleisch, The role of Ni in modifying the order of the phase transition of $La(Fe,Ni,Si)_{13}$, Acta Materialia 160 (2018) 137-146.